Macromolecular Chemistry and Physics
www.mcp-journal.de

Revealing the Monomer Gradient of Polyether Copolymers Prepared Using *N*-Heterocyclic Olefins: Metal-Free Anionic versus Zwitterionic Lewis Pair Polymerization

Erik Kersten, Olga Linker, Jan Blankenburg, Manfred Wagner, Patrick Walther, Stefan Naumann, and Holger Frey**

***N*-Heterocyclic olefin (NHO)-based polymerization pathways for the copolymerization of ethylene oxide (EO) and propylene oxide (PO) are investigated in detail. Employing in situ ^{1}H NMR spectroscopy, both an organocatalytic, anionic polymerization setup (system A) and a zwitterionic, Lewis pair-type approach (system B) are studied comparatively. The obtained kinetics data are fitted to the non-terminal model (Jaacks and Ideal Integrated) and terminal Mayo–Lewis model (Meyer Lowry) to determine the reactivity ratios, revealing striking differences in copolyether microstructure and achievable molar masses. While for the metal-free catalysis (system A) reactivity ratios of $r_{EO} = 3.4$ and $r_{PO} = 0.30$ are found, indicating a soft gradient structure, the presence of $Mg(HMDS)_2$ (system B) entails exclusively zwitterionic propagation. This results in enhanced selectivity, displaying corresponding parameters of $r_{EO} = 7.9$ and $r_{PO} = 0.13$, in line with the proposed monomer-activated mechanism. The block-like, strongly tapered copolyether microstructure is also reflected in the thermal properties, showing a melting point for the latter sample and much higher molar masses (M_n >50 000 g mol^{-1}). Notably, this study not only identifies capable polymerization systems for EO/PO, but also underlines that via in situ ^{1}H NMR kinetics key questions regarding the polymerization mechanism can be illuminated quickly and reliably, simplifying access to essential structure-property relations.**

1. Introduction

Aliphatic polyethers are commonly prepared by the ring-opening polymerization (ROP) of epoxide monomers and are a highly established class of industrial polymers, finding use in a broad range of applications.[1] The most important epoxide monomers are ethylene oxide (EO) and propylene oxide (PO), which are converted to their corresponding (co)polymers on a megaton scale.[2] The water soluble poly(ethylene oxide) (PEO, often also called poly(ethylene glycol, PEG) is semi-crystalline and employed in numerous pharmaceutical and medical applications, since it is non-toxic, biocompatible, and inexpensive.[1] Poly(propylene oxide) (PPO) is a flexible, hydrophobic, and amorphous polymer with a low glass transition temperature of −73 °C.[3] PPO plays a key role as soft segment in polyurethane foams and as an additive in lubricants.[4–6] ABA triblock copolymers composed of PEO-*b*-PPO-*b*-PEO are known as *Poloxamers* or *Pluronics* and are applied as non-ionic surfactants,[7–9] for hydrogels,[10–12] as nanotemplates[13,14] or in drug delivery systems.[15,16] Polyether topology and the generation of functionalized structures is of enduring interest in this regard.[17–19]

A variety of polymerization methods such as the conventional anionic ROP (AROP), coordination polymerization, and cationic polymerization can be used to synthesize polyether (co)polymers, facilitated by the notable ring strain of epoxides (115 kJ mol^{-1} for EO) as a driving force.[20] The major challenge in the (co)polymerization of PO is a severe limitation of molar mass, a consequence of

E. Kersten, O. Linker, J. Blankenburg, H. Frey
Institute of Organic Chemistry
Johannes Gutenberg University Mainz
55128, Duesbergweg 10–14 Mainz, Germany
E-mail: hfrey@uni-mainz.de

O. Linker, J. Blankenburg
Graduate School Materials Science in Mainz
Johannes Gutenberg University Mainz
55128, Staudinger Weg 9 Mainz, Germany

M. Wagner
Max-Planck-Institute for Polymer Research
Ackermannweg 10, 55128 Mainz, Germany

P. Walther, S. Naumann
Institute of Polymer Chemistry
University of Stuttgart
Pfaffenwaldring 55, 70569 Stuttgart, Germany
E-mail: stefan.naumann@ipoc.uni-stuttgart.de

DOI: 10.1002/macp.202300097

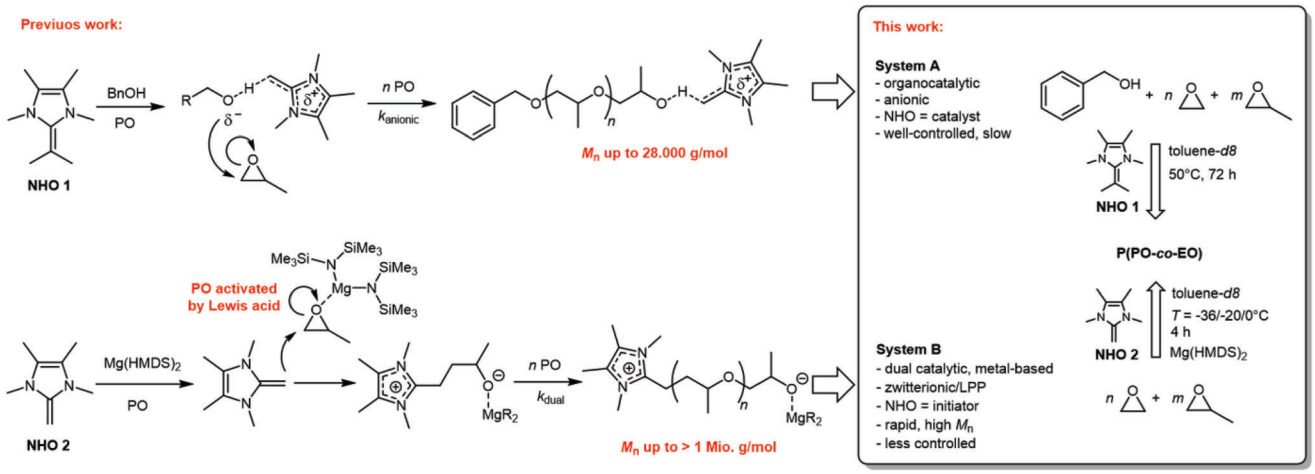

Figure 1. Previous work on PO homopolymerization using NHO organocatalysis (anionic, system A) and NHO dual catalysis (zwitterionic LPP, system B) and the corresponding EO/PO copolymers investigated in this work.

chain transfer reactions that also entail the formation of allyl-type end groups.[1] This limitation has inspired the development of advanced (organo)catalysts.[21–27] For example, Taton et al. introduced the application of *N*-heterocyclic carbenes (NHCs) as organocatalysts for the metal free polyether synthesis. The polymerization of PO was realized, however, the absence of allyl species was only ensured for molecular weights below 4 500 g mol^{-1}.[28] The same group reported the synthesis of α,ω-heterodifunctionalized poly(ethylene oxide)s using NHCs as organocatalysts.[29] In 2015 Naumann and Dove described the preparation of well-defined PPO using *N*-heterocyclic olefins (NHOs) as organocatalysts and benzyl alcohol as an initiator, along an anionic polymerization pathway.[30] NHO catalysis, which relies on the strong polarity of the olefinic bond,[31–33] is a powerful technique to largely suppress the aforementioned transfer reaction, also enabling the controlled preparation of reverse *Pluronics* structures ($Đ_M$ = 1.02–1.03, M_n up to 28 000 g mol^{-1}).[34] However, in the latter case, functional PEG was employed for polymer synthesis, so the conversion of EO has never been investigated; also, the preparation of truly high-molar mass polyether remained an unmet challenge with this specific organocatalytic, anionic polymerization system.

To address this issue, Naumann et al. recently reported a dual catalytic strategy based on NHOs and magnesium bis(hexamethyldisilazide) ($Mg(HMDS)_2$) as Lewis acidic catalyst for the synthesis of PPO with high molar masses without the requirement of an alcohol initiator.[35] The presence of the metal-based Lewis acid transforms the polymerization mechanism from anionic to exclusively zwitterionic, as evidenced by MALDI-ToF MS and NMR analysis. Notably, the NHO operates as initiator in this case. Thereby, $Mg(HMDS)_2$ fulfills the dual role of monomer activator and chain end-complexing agent, rendering the whole mechanism a zwitterionic Lewis pair polymerization (LPP).[36] Transfer reactions are quantitatively suppressed since the basicity of the propagating alkoxides is strongly reduced—most likely to such a degree that it can only react with activated monomer. Consequently, this technique enables access to high-molar mass PPO ($M_n > 10^6$ g mol^{-1}, DP > 20 000). The proposed pathways are depicted in **Figure 1**.

While this switch of polymerization mechanism and the ensuing change in obtainable polyether molar masses is conceptually intriguing, a number of questions has remained unanswered to date: i) Can the commercially important EO be copolymerized using NHO-based catalysis as well? ii) Coherently, if such EO/PO copolymerization is successful, what type of microstructure will result? Since the distribution pattern of the respective repeat units (i.e., blocky or statistical) is decisive for polymer properties and the relative ratio of primary/secondary hydroxyl end groups, the latter is no trivial question but rather one of technical and practical importance,[37–40] which is obviously also true for other types of epoxide monomers.[41,42]

In contrast, the conventional AROcP for the synthesis of P(PO-*co*-EO) has been comprehensively investigated long since and the corresponding reactivity ratios were determined to be r_{EO} = 2.8 and r_{PO} = 0.25.[43,44] Recently, Frey and co-workers reported that the P(PO-*co*-EO) gradient is defined by the polymerization method.[45] Thus, reactivity ratios of r_{EO} = 6.4 and r_{PO} = 0.16 for the copolymerization under monomer-activated AROcP conditions (using triisobutyl aluminum/ tetraoctylammonium bromide) were calculated by the ideal integrated fit method, while the copolymerization using double metal cyanide (DMC) catalysts revealed a remarkable, reversed monomer gradient with r_{EO} = 0.42 and r_{PO} = 2.4. This observation suggested that the different NHO-based mechanisms might also entail interesting selectivity patterns. Hence, in the following, the copolymerization of EO and PO is investigated in detail, using advanced in situ ^{1}H NMR monitoring of this highly relevant monomer combination.

2. Results and Discussion

Reactivity ratios can be extracted from the in situ ^{1}H NMR measurements by fitting a copolymerization model to the monomer conversion data. The simplest model to describe a copolymerization was introduced by Wall in 1941.[46] This non-terminal model suggests the same selectivity of the active polymer chain ends. In 1944 the terminal model was introduced, which considers the influence of the terminal polymer chain end. This leads to reactivity ratios with the product $r_1 r_2$ unequal to one.[47–50]

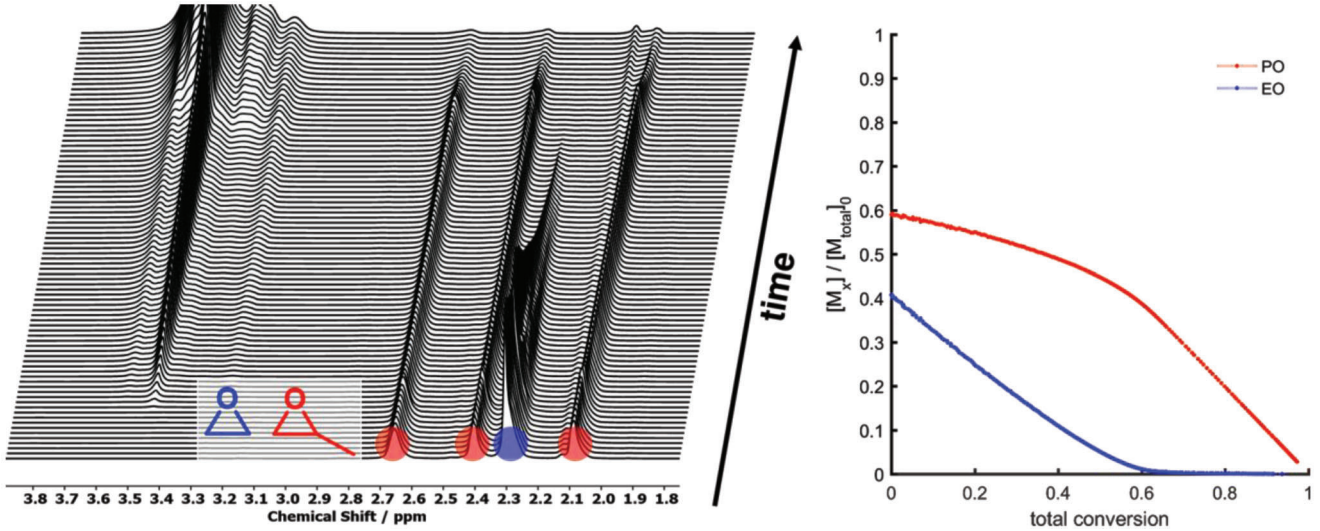

Figure 2. In situ ^{1}H NMR (500 MHz, toluene-d_8) spectra of the copolymerization of PO and EO using the dual NHO/Mg(HMDS)$_2$ setup at −20 °C (left); corresponding monomer concentration as a function of total conversion (right).

In 2015, Lynd et al. reported a derivation of the Wall equation of the non-terminal model[51] and in 2019 the same group presented a process to determine whether non-terminal or terminal models are best suited to describe a given copolymerization, with a focus on using the least degree of complexity to avoid overfitting phenomena.[52] In the study presented here, the kinetic data were fitted to the non-terminal model according to Jaacks[50] and the ideal integrated equation[45] as well as the terminal model according to the Meyer–Lowry equation,[53] respectively. The ideal integrated equation (II-fit) allows for the direct comparison of the non-terminal and terminal model and can thereby prevent the aforementioned overfitting by choosing the least complex model that can accurately describe the data.

The copolymerization behavior of PO and EO using NHO organocatalysis (system A) and dual catalysis (system B, see Figure 1) was directly compared by in situ ^{1}H NMR measurements. Note that different NHOs were employed in the respective setups: while the anionic, metal-free process relied on **NHO 1**, a strongly basic, sterically encumbered compound optimized for proton abstraction, in the dual-catalytic process **NHO 2** was applied, which is a capable nucleophile.[33] In both cases, toluene-d_8 was employed as solvent.

Monomer conversion was monitored by focusing on the decreasing proton signals of the epoxides (exemplified in **Figure 2**), and 500–1000 individual ^{1}H NMR spectra were recorded for a single kinetic experiment. This copious amount of data was used to calculate the monomer concentration as a function of total conversion or reaction time. Indeed, drastic variations in the copolymerization kinetics reflected the differences in the underlying polymerization mechanisms.

In case of NHO organocatalysis (system A, Figure 1) at 50 °C, faster conversion of EO compared to PO was observed (Figure S3, Supporting Infomation), in agreement with expectation for an AROcP. Both the II fit and the ML fits have been applied to the experimental kinetics data (see **Figure 3**). The fits of II and ML to the experimental data are very similar. We suggest that the ideal model is sufficient for the description of this copolymerization. Therefore, the reactivity ratios were determined by the II-fit with $r_{EO} = 3.4$ and $r_{PO} = 0.30$. The Jaacks fit, which is also based on the non-terminal model, is depicted in Figure S6 (Supporting Information) and gave the same reactivity ratios of $r_{EO} = 3.4$ and $r_{PO} = 0.30$. The determined reactivity ratios were comparable to those of conventional AROcP ($r_{EO} = 2.8$ and $r_{PO} = 0.26$).[44] These results strongly support the proposed oxyanionic pathway suggested by Naumann and Dove.[30] The reaction time was set to 70 h to achieve full conversion of EO.

Fits of an exponential decay of the monomer concentrations gave the half-lives. Due to the very long half-lives of PO with 35 and 10 h for EO, there were still traces of unreacted PO left even after a reaction time of 8 days (see Figure S11 Supporting Information). The obtained copolymer was isolated and comprehensively characterized by additional NMR spectroscopy (see Figures S12–S16, Supporting Information).

Next, the copolymerization via the zwitterionic species (system B, Figure 1) was performed using **NHO 2** and Mg(HMDS)$_2$. In accordance with literature no alcohol was added to the setup, which would otherwise inhibit efficient polymerization.[35] For an effective monitoring of the ^{1}H NMR data the temperature was first set to −36 °C (see Figure S17, Supporting Information). After a reaction time of 6 h the total conversion was ≈30% (Figure S18, Supporting Information). The half-lives of PO (32 h) and EO (4 h) were higher than expected, perhaps reflecting the effect of dilution by the deuterated solvent, considering that LPP is inherently vulnerable to a lower catalyst concentration.[36] In order to study the temperature influence on this copolymerization, further experiments at different temperatures were performed. A second kinetics measurement was initiated, and the reaction temperature was raised to 0 °C to accelerate the polymerization. The copolymerization at 0 °C was very fast, and monomer was already consumed directly after the set-up process (Figure S35, Supporting Information). Under these conditions, EO was completely incorporated after 5 min, and quantitative conversion was reached after 20 min. Based on these results, an intermediate reaction temperature of $T = -20$ °C was chosen to access kinetics

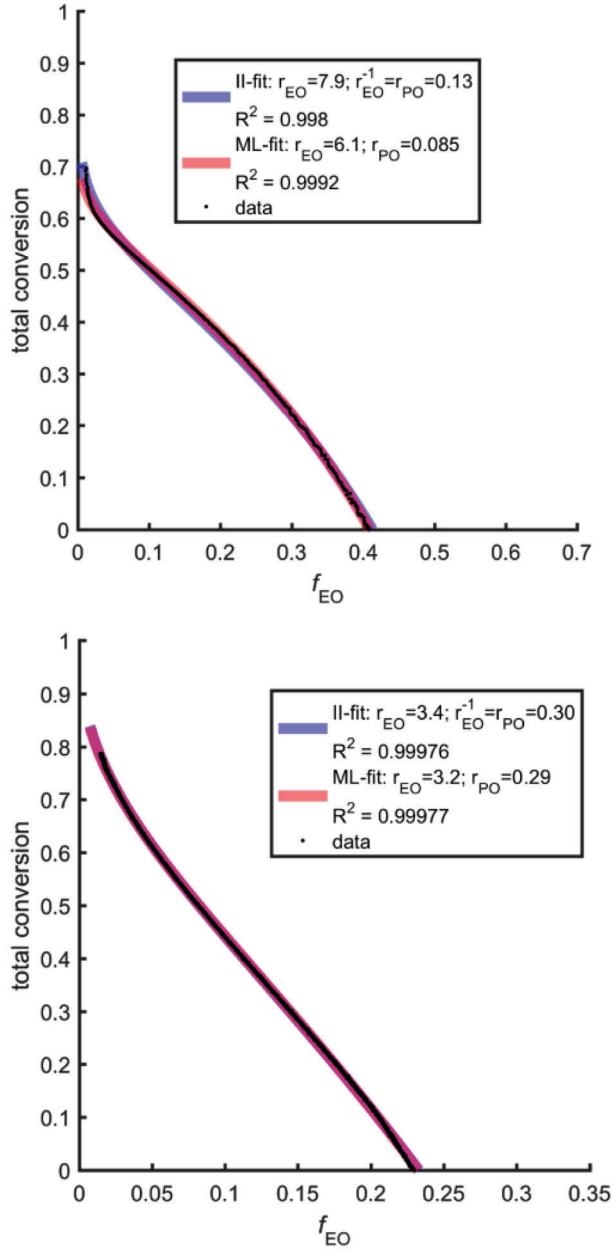

Figure 3. Integrated ideal fit (II-fit) with resulting reactivity ratios, top: dual NHO/$Mg(HMDS)_2$ catalysis (zwitterionic) at −20 °C, and bottom: NHO organocatalysis at 50 °C (anionic).

data suitable for determining reactivity ratios. It should thus be underlined that the polymerization runs smoothly in benign temperature regimes (0–60 °C)[35] and the low reaction temperature was chosen for experimental reasons only. A comparison of the calculated reactivity ratios by Jaacks, II and ML is given in Table S1 (Supporting Information). The determined half-lives are summarized in Table S2 (Supporting Information). For NHO dual catalysis at −20 °C the fits differ stronger compared to NHO organocatalysis, which becomes apparent in the fit for high conversion. However, in this section the experimental errors are highest due to low remaining comonomer concentrations. We therefore consider the reactivity ratios determined with r_{EO} = 7.9 and r_{PO} = 0.13 by the II fit as being most reliable and propose that the deviation for ML (r_{EO} = 6.1 and r_{PO} = 0.085) is a result of overfitting. The determination of the reactivity ratios according to Jaacks is depicted in Figure S33 (Supporting Information). Again, similar reactivity ratios were calculated. These results suggest no significant influence of temperature on the reactivity ratios. Interestingly, the values obtained are close to the ones reported for monomer-activated AROcP (r_{EO} = 6.4 and r_{PO} = 0.16, via $^{i}Bu_3Al$).[45] This similarity may well reflect the mechanistic parallels to the NHO-based zwitterionic LPP mechanism, where likewise monomer activation occurs (via $Mg(HMDS)_2$). The close interaction of epoxide and coordinating Lewis acid renders this mechanism more monomer selective, because stereoelectronic factors, such as the presence of the additional methyl group in PO, can directly affect the relative concentration of activated PO in relation to activated EO. It is proposed that this engenders a more pronounced gradient in the copolyether (see also discussion below). Mechanistically, this means that the monomer-Lewis acid interactions are the most promising tuning site for further emphasizing such selectivities.[36] These features, and the higher polymerization rates and achievable molar masses, are fundamentally different from conventional AROcP.

The major obstacle for the preparation of high-molecular weight PPO is the abstraction of the slightly acidic proton of the PO monomer during propagation, resulting in the formation of allyl alkoxides (transfer-to-monomer), which are themselves able to initiate chain growth.[1,24] Notably in this regard, the polymers obtained from both NHO catalytic systems were well-defined and practically free of this side reaction, which is crucial concerning their application, for example, as a polyol component for polyurethane chemistry.[54] The absence of any allyl species is documented for NHO organocatalysis (Figure S12, Supporting Information) and for dual NHO catalysis (Figures S45–S47, Supporting Information).

An investigation of the controlled character of both setups was also performed by logarithmic plotting of the concentration $\ln([M]_0/[M])$ over time. Based on the assumption that side reactions like transfer-to-monomer or termination reactions are sufficiently suppressed and the concentration of the active chain ends is constant, pseudo first order kinetics, that is, a linear correlation, can be expected for system A.[55] The corresponding plots for NHO organocatalysis at 50 °C and NHO dual catalysis at −20 °C are shown in **Figure 4**. In the case of the AROcP-like NHO catalysis (system A) a linear function of the logarithmic concentration $\ln([M]_0/[M])$ over time was observed after complete initiation. However, an induction time of ca.10 h can be observed, and after that point the slope remains constant, implying that quantitative initiation was achieved only after 10 h (Figure 4, bottom), potentially reflecting the transition from primary (BnO^-) to secondary alkoxide species.

This almost perfectly linear behavior further indicated the controlled character of NHO organocatalysis, which is underpinned by a narrow molecular weight distribution ($Đ_M$ = 1.13), despite the lack of stirring (see Figure S8, Supporting Information). In contrast, clearly non-linear behavior was detected for the dual catalytic approach (system B, Figure 4, top). This setup with its zwitterionic species is comparable to the monomer-activated AROcP reported by Carlotti and Deffieux.[56] The increasing slope

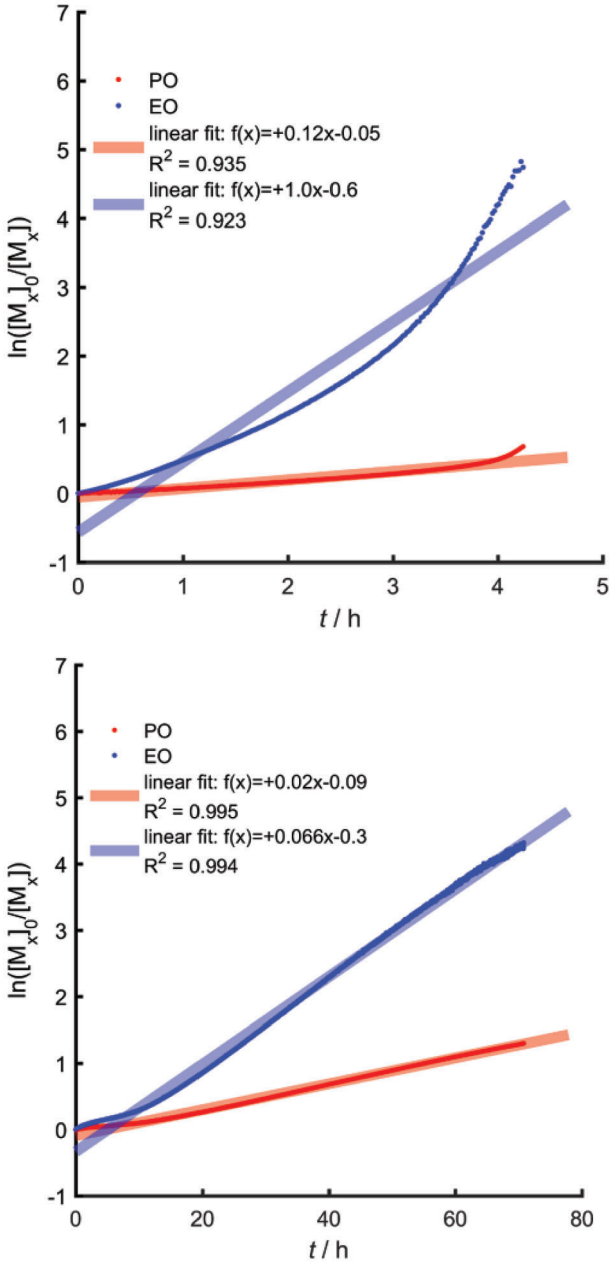

Figure 4. Logarithmic plot of monomer consumption over time. Top: dual NHO/$Mg(HMDS)_2$ catalysis (zwitterionic LPP, system B) at −20 °C; bottom: NHO organocatalysis at 50 °C (anionic, system A).

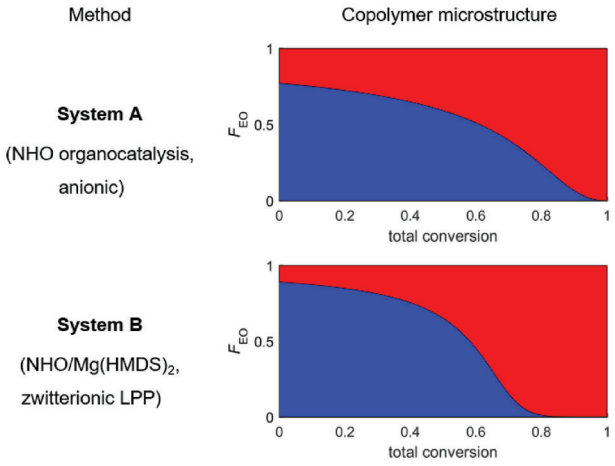

Figure 5. Copolymer composition as a function of total conversion of an equimolar fraction of PO (red) and EO (blue).

of the datapoints suggests that either the rate of the polymerization or the concentration of active chains increased during the copolymerization. This observation was already reported by our group for the copolymerization of EO and PO using the iBu$_3$Al catalyst[45,57] and is in this case in excellent accordance with literature. For the NHO copolymerization we tentatively explain this increase by a slowly growing number of active chains due to the rather slow zwitterion formation (initiation).[35] The molar mass distribution of the dual NHO catalyzed copolymers consequently was somewhat broader, but still moderate with $Đ_M$ ≈1.3 and M_n >40 000 g mol^{-1}, despite the lack of stirring in the NMR tube (see Figure S23, Supporting Information). Note that $Mg(HMDS)_2$ can potentially act as a purifier for the polymerization setup by reacting with undesired protic impurities. The high molar masses are possible because transfer-to-monomer is suppressed, and protic quenching agents are removed.

The copolymer composition can be calculated as a function of the conversion, based on the experimental reactivity ratios.[58,59] In the case of a living copolymerization the total conversion is equivalent to the relative position in the polymer chain. According to the above discussions, NHO catalysis shows sufficiently controlled character for this analysis to be applicable. The calculated microstructure based on the determined reactivity ratios is shown in **Figure 5** for an equimolar fraction of PO and EO, both under the conditions of NHO organocatalysis and dual catalysis. Very recently it was demonstrated that the microstructure of P(PO-*co*-EO) copolymers can be specifically adjusted by the choice of the polymerization method using conventional AROcP, monomer activated AROcP and DMC catalysis.[45] Interestingly, as discussed above, the determined reactivity ratios for NHO organocatalysis (system A) were very similar to those of conventional AROcP,[44] and coherently the comonomer gradient is also quite similar. PO is less reactive in conventional AROcP, and a weak gradient is obtained (Figure 5, top).[44] In comparison, the reactivity ratios in NHO dual catalysis with added $Mg(HMDS)_2$ were strikingly different. In accordance with the monomer-activated AROcP the gradient is now much more pronounced. EO incorporation is more likely at early stages, and PO consumption is accordingly favored for high conversion. A summary of the different polymerization methods and the corresponding copolymer microstructures is given in Table S3 (Supporting Information).

The thermal properties of the copolymers were studied by differential scanning calorimetry (DSC) in order to assess the effect of the gradient structure. The glass transition temperature (T_g) of PEO homopolymer is −60 °C and the melting temperature is 65 °C.[1] The PPO homopolymer exhibits a T_g of −73 °C.[3] The NHO organocatalysis-derived P(PO-*co*-EO) copolymer displays a T_g of −72 °C, and no melting point is observed, which is due to the low molecular weight in combination with the soft gradient

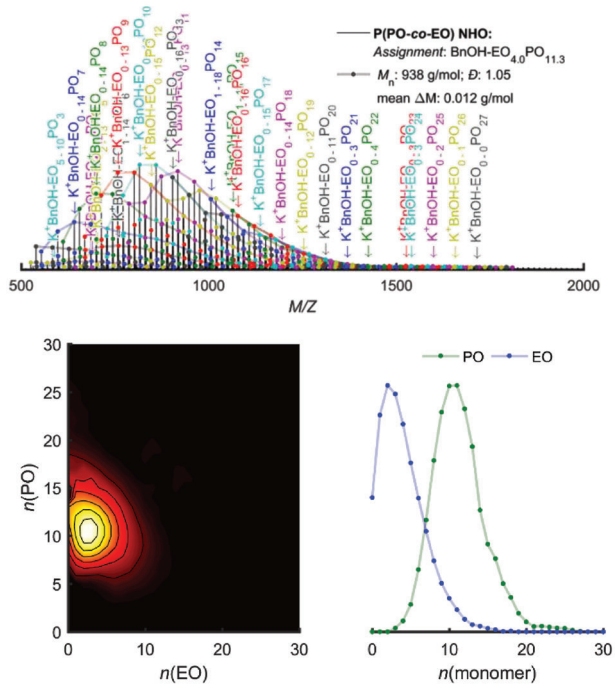

Figure 6. Top: MALDI-ToF mass spectra with assigned peaks of P(PO-*co*-EO) copolymer using NHO AROcP at 50 °C. Bottom left: 2D-composition. Bottom right: representation of the monomer distribution in 2D.

(SEC M_n = 810 g mol^{-1}, see Figure S8, Supporting Information). A segment length of ≈13 EO units is necessary for crystallization of the PEO segments.[60] For dual NHO catalysis a T_g of −68 °C was determined. Significantly, a melting temperature of −5 °C, indicating crystallizable, pure PEG-segments, was also found, underlining the strong gradient formed using this type of polymerization catalysis.

MALDI-ToF MS analysis of the organicatalytically derived P(PO-*co*-EO) copolymer confirmed the controlled nature of this polymerization technique and further illustrates the formation of well-defined copolymers (see **Figure 6**). The obtained mass spectra showed copolymer chains exclusively initiated by benzyl alcohol and all mass peaks could be assigned to a linear combination of the comonomers PO and EO.[59] The assignments in the mass spectrum can be depicted as a 2D map of the copolymer composition.[61,62]

These results corroborate the proposed living character of the NHO catalysis and the similarity to the conventional AROcP, confirming claims by Naumann and Dove.[30] The mass spectra proved the formation of copolymers, and the presence of a blend of homopolymers can be ruled out. Diffusion-ordered spectroscopy (DOSY) showed one diffusion coefficient for the P(PO-*co*-EO) copolymer (see Figure S10, Supporting Information). In analogy, MALDI-ToF MS analysis was performed for the high molecular weight P(PO-*co*-EO) copolymer from dual NHO catalysis (see Figure S41, Supporting Information). As expected, the resolution was insufficient to evaluate distinct mass peaks, but the calculated average molecular weight of 51 000 g mol^{-1} was in accordance with expectation and the SEC traces (see Figure S23, Supporting Information). Again, DOSY measurements showed a single diffusion coefficient for all three copolymers (obtained at T = −36, −20, and 0 °C, see Figures S42–S44, Supporting Information).

3. Conclusion

In summary, the first successful copolymerization of PO and EO via NHO organo- and dual catalysis conditions is reported. Especially the dual, Mg(II)-assisted approach (system B) represents a viable strategy to synthesize high-molar mass P(PO-*co*-EO) copolymers with molecular weights >50 000 g mol^{-1}, exceeding the scope of classical AROcP. A detailed study of the copolymer composition with respect to the polymerization conditions has been performed. The in situ ^{1}H NMR kinetics data were fitted to the ideal integrated equation, the Jaacks equation, and the Meyer–Lowry equation for the established terminal copolymerization model. As expected, the calculated reactivity ratios differ, depending on the applied copolymerization model. In NHO organocatalysis (system A), fits of Ideal Integrated (II) and Meyer–Lowry (ML) equation were very similar (r_{EO} = 3.4/r_{PO} = 0.30, and r_{EO} = 3.2/r_{PO} = 0.29, respectively), which underpins the proposed anionic mechanism of the NHO **1** catalyst. In excellent accordance with the postulated zwitterionic LPP mechanism,[35] the reactivity of the epoxide monomers drastically changed in the presence of Mg(HMDS)$_2$ and absence of alcohol initiators. The determined reactivity ratios with r_{EO} = 7.9 and r_{PO} = 0.13 for the II fit are in the range identified for other monomer-activated AROcP methods, thus further substantiating the proposed mechanism involving epoxide activation via coordination to the magnesium catalyst. Taken together, these results enable fundamental understanding of the mechanism of the NHO-catalyzed ROP and the design of polyether structures with predefined monomer gradient, which is of relevance for tailored polyether products, both in industry as well as in academic research.

Supporting Information

Supporting Information is available from the Wiley Online Library or from the author.

Acknowledgements

The authors thank Stefan Spang and Petra Raeder for technical assistance. O.L. and J.B. thank the Graduate School "Materials Science in Mainz (MAINZ)" for financial support. S.N. gratefully acknowledges funding by the Deutsche Forschungsgemeinschaft (DFG, German Research Foundation) – Project-ID 358283783 – SFB 1333/2 2022.

Open access funding enabled and organized by Projekt DEAL.

Conflict of Interest

The authors declare no conflict of interest.

Data Availability Statement

The data that support the findings of this study are available in the supporting information of this article.

Keywords

copolymerization, in situ techniques, Lewis pairs, organocatalysis, polyethers

Received: April 4, 2023
Revised: May 8, 2023
Published online: May 31, 2023

[1] J. Herzberger, K. Niederer, H. Pohlit, J. Seiwert, M. Worm, F. R. Wurm, H. Frey, *Chem. Rev.* **2016**, *116*, 2170.
[2] T. A. Nijhuis, M. Makkee, J. A. Moulijn, B. M. Weckhuysen, *Ind. Eng. Chem. Res.* **2006**, *45*, 3447.
[3] G. P. Johari, A. Hallbrucker, E. Mayer, *J. Polym. Sci., Part B: Polym. Phys.* **1988**, *26*, 1923.
[4] X. Paredes, A. S. Pensado, M. J. P. Comuñas, J. Fernández, *J. Chem. Eng. Data* **2010**, *55*, 4088.
[5] H.-W. Engels, H.-G. Pirkl, R. Albers, R. W. Albach, J. Krause, A. Hoffmann, H. Casselmann, J. Dormish, *Angew. Chem., Int. Ed.* **2013**, *52*, 9422.
[6] F. T. Hong, V. Ladelta, R. Gautam, S. M. Sarathy, N. Hadjichristidis, *ACS Appl Polym Mater* **2021**, *3*, 3811.
[7] I. R. Schmolka, *J. Amer. Oil Chem. Soc.* **1977**, *54*, 110.
[8] P. Alexandridis, T. Alan Hatton, *Colloids Surf., A* **1995**, *96*, 1.
[9] P. Alexandridis, *Curr. Opin. Colloids Interface Sci.* **1997**, *2*, 478.
[10] B. Jeong, S. W. Kim, Y. H. Bae, *Adv. Drug Delivery Rev.* **2012**, *64*, 154.
[11] Y. Qiu, K. Park, *Adv. Drug Delivery Rev.* **2001**, *53*, 321.
[12] F. Markus, J. R. Bruckner, S. Naumann, *Macromol. Chem. Phys.* **2020**, *221*, 1900437.
[13] Y. Meng, D. Gu, F. Zhang, Y. Shi, L. Cheng, D. Feng, Z. Wu, Z. Chen, Y. Wan, A. Stein, D. Zhao, A. Stein, *Chem. Mater.* **2006**, *18*, 4447.
[14] F. Markus, C. Vogler, J. R. Bruckner, S. Naumann, *ACS Appl. Nano Mater.* **2021**, *4*, 3486.
[15] E. V. Batrakova, A. V. Kabanov, *J. Controlled Release* **2008**, *130*, 98.
[16] A. Pitto-Barry, N. P. E. Barry, *Polym. Chem.* **2014**, *5*, 3291.
[17] S. I. E. Kim, Y. U.-R. I. Lee, M. Kim, E. Seo, H.-J. Paik, J. C. Kim, J. I.-E. Jeong, Y. I. L. Park, B.-S. U. Kim, S.-H. O. Lee, *Polym. Chem.* **2022**, *13*, 1243.
[18] J. Park, Y. Yu, J. W. Lee, B.-S. U. Kim, *Macromolecules* **2022**, *55*, 5448.
[19] T. He, Y. Wang, A. Narumi, L. Xu, S.-I. Sato, X. Shen, T. Kakuchi, *Polymers* **2021**, *13*, 3873.
[20] T. Dudev, C. Lim, *J. Am. Chem. Soc.* **1998**, *120*, 4450.
[21] W. N. Ottou, H. Sardon, D. Mecerreyes, J. Vignolle, D. Taton, *Progr. Polym. Sci.* **2016**, *56*, 64.
[22] L. Dentzer, C. Bray, S. Noinville, N. Illy, P. Guégan, *Macromolecules* **2015**, *48*, 7755.
[23] M. Fèvre, J. Pinaud, Y. Gnanou, J. Vignolle, D. Taton, *Chem. Soc. Rev.* **2013**, *42*, 2142.
[24] P. Walther, C. Vogler, S. Naumann, *Synlett* **2020**, *31*, 641.
[25] G.-W. Yang, Y.-Y. Zhang, G.-P. Wu, *Acc. Chem. Res.* **2021**, *54*, 4434.
[26] C. Zhang, X. Geng, X. Zhang, Y. Gnanou, X. Feng, *Progr. Polym. Sci.* **2023**, *136*, 101644.
[27] S. Naumann, *Polym. Chem.* **2023**, *14*, 1834.
[28] J. Raynaud, W. N. Ottou, Y. Gnanou, D. Taton, *Chem. Commun.* **2010**, *46*, 3203.
[29] J. Raynaud, C. Absalon, Y. Gnanou, D. Taton, *Macromolecules* **2010**, *43*, 2814.
[30] S. Naumann, A. W. Thomas, A. P. Dove, *Angew. Chem., Int. Ed.* **2015**, *54*, 9550.
[31] R. D. Crocker, T. V. Nguyen, *Chem. - Eur. J.* **2016**, *22*, 2208.
[32] M. M. D. Roy, E. Rivard, *Acc. Chem. Res.* **2017**, *50*, 2017.
[33] S. Naumann, *Chem. Commun.* **2019**, *55*, 11658.
[34] A. Balint, M. Papendick, M. Clauss, C. Müller, F. Giesselmann, S. Naumann, *Chem. Commun.* **2018**, *54*, 2220.
[35] P. Walther, A. Krauß, S. Naumann, *Angew. Chem., Int. Ed.* **2019**, *58*, 10737.
[36] M. L. Mcgraw, E. Y.-X. Chen, *Macromolecules* **2020**, *53*, 6102.
[37] F. Heatley, Y. Luo, J. Ding, R. H. Mobbs, C. Booth, *Macromolecules* **1988**, *21*, 2713.
[38] U. Tsoler, *Handbook of Detergents: Part F*, (Eds: E. Santacesaria, M. Di Serio, R. Tesser), M. Dekker, New York **2009**.
[39] R. Tesser, E. Santacesaria, *Ind. Eng. Chem. Res.* **2021**, *60*, 16619.
[40] V. St-Onge, S. Rochon, J.-C. Daigle, A. Soldera, J. P. Claverie, *Angew. Chem., Int. Ed.* **2021**, *60*, 25897.
[41] O. Linker, J. Blankenburg, K. Maciol, M. Bros, H. Frey, *Macromolecules* **2020**, *53*, 3524.
[42] V. Müller, R. Matthes, M. Wagner, M. Bros, P. Dreier, H. Frey, *Polym. Chem.* **2023**, *14*, 2599.
[43] Y. Deng, J. Ding, G. Yu, R. H. Mobbs, F. Heatley, C. Price, C. Booth, *Polymer* **1992**, *33*, 1959.
[44] J. Ding, F. Heatley, C. Price, C. Booth, *Eur. Polym. J.* **1991**, *27*, 895.
[45] J. Blankenburg, E. Kersten, K. Maciol, M. Wagner, S. Zarbakhsh, H. Frey, *Polym. Chem.* **2019**, *10*, 2863.
[46] F. T. Wall, *J. Am. Chem. Soc.* **1941**, *63*, 1862.
[47] T. Alfrey, G. Goldfinger, *J. Chem. Phys.* **1944**, *12*, 205.
[48] F. R. Mayo, F. M. Lewis, *J. Am. Chem. Soc.* **1944**, *66*, 1594.
[49] F. T. Wall, *J. Am. Chem. Soc.* **1944**, *66*, 2050.
[50] V. Jaacks, *Makromol. Chem.* **1972**, *161*, 161.
[51] B. S. Beckingham, G. E. Sanoja, N. A. Lynd, *Macromolecules* **2015**, *48*, 6922.
[52] N. A. Lynd, R. C. Ferrier, B. S. Beckingham, *Macromolecules* **2019**, *52*, 2277.
[53] V. E. Meyer, G. G. Lowry, *J. Polym. Sci., Part A: Gen. Pap.* **1965**, *3*, 2843.
[54] M. Ionescu, *Chemistry and Technology of Polyols for Polyurethanes*, iSmithers Rapra Technology, Shropshire, U.K. **2005**.
[55] J. Qiu, B. Charleux, K. Matyjaszewski, *Progr. Polym. Sci.* **2001**, *26*, 2083.
[56] V. Rejsek, D. Sauvanier, C. Billouard, P. Desbois, A. Deffieux, S. Carlotti, *Macromolecules* **2007**, *40*, 6510.
[57] K. Sakakibara, K. Nakano, K. Nozaki, *Chem. Commun.* **2006**, 3334.
[58] I. Skeist, *J. Am. Chem. Soc.* **1946**, *68*, 1781.
[59] J. Blankenburg, M. Wagner, H. Frey, *Macromolecules* **2017**, *50*, 8885.
[60] O. Olabisi, K. P. Adewale, *Handbook of Thermoplastics*, 2nd ed., CRC Press Taylor, Boca Raton, FL **2016**.
[61] G. J. Van Rooij, M. C. Duursma, C. G. De Koster, R. M. A. Heeren, J. J. Boon, P. J. W. Schuyl, E. R. E. Van Der Hage, *Anal. Chem.* **1998**, *70*, 843.
[62] G. Wilczek-Vera, P. O. Danis, A. Eisenberg, *Macromolecules* **1996**, *29*, 4036.

